High-quality single crystal growth and the Fermi surface property of uranium and cerium compounds

2003 J. Phys.: Condens. Matter 15 S1903

(http://iopscience.iop.org/0953-8984/15/28/301)

INSTITUTE OF PHYSICS PUBLISHING JOURNAL OF PHYSICS: CONDENSED MATTER

J. Phys.: Condens. Matter **15** (2003) S1903–S1909 PII: S0953-8984(03)62575-0

High-quality single crystal growth and the Fermi surface property of uranium and cerium compounds

Yoshichika Ōnuki[1,2], Yoshinori Haga[2], Etsuji Yamamoto[2], Yoshihiko Inada[1], Rikio Settai[1], Hiroshi Yamagami[3] and Hisatomo Harima[4]

[1] Graduate School of Science, Osaka University, Toyonaka, Osaka 560-0043, Japan
[2] Advanced Science Research Center, Japan Atomic Energy Research Institute, Tokai, Ibaraki 319-1195, Japan
[3] Faculty of Science, Department of Physics, Kyoto Sangyo University, Kita-ku, Kyoto 603-8555, Japan
[4] Institute of Scientific and Industrial Research, Osaka University, Ibaraki, Osaka 567-0047, Japan

Received 12 November 2002
Published 4 July 2003
Online at stacks.iop.org/JPhysCM/15/S1903

Abstract

We present descriptions of the single crystal growth of uranium and cerium compounds via the Czochralski-pulling, self-flux and vapour transport methods. We also report the results of de Haas–van Alphen experiments and energy band calculations for a Hill-plot rule of UX_3 (X: Si, Ge, Sn and Pb), heavy fermion systems of UPt_3 and UPd_2Al_3, quasi-two-dimensional electronic states of $UPtGa_5$, UX_2 (X: Bi, Sb, As, P) and $CeCoIn_5$, characteristic semimetals of UC and $CeAgSb_2$, and quantum critical phenomena in UGe_2 and $CeRh_2Si_2$.

1. Introduction

Uranium and cerium compounds exhibit a variety of properties such as magnetic, charge and quadrupolar ordering, heavy fermions, small magnetic moments, Kondo insulators and unconventional superconductivity [1]. In this paper we present the Fermi surface property of uranium compounds, together with that of typical cerium compounds, via de Haas–van Alphen (dHvA) experiments and energy band calculations. Uranium compounds can be classified into five categories based on characteristic features:

(1) Hill-plot rule of UX_3 (X: Si, Ge, Sn, Pb),
(2) heavy fermion systems of UPt_3 and UPd_2Al_3,
(3) quasi-two-dimensional electronic states of $UPtGa_5$ and UX_2 (X: Bi, Sb, As, P), together with $CeCoIn_5$,
(4) semimetal behaviour of UC and $CeAgSb_2$, and
(5) quantum critical phenomena in UGe_2 and $CeRh_2Si_2$.

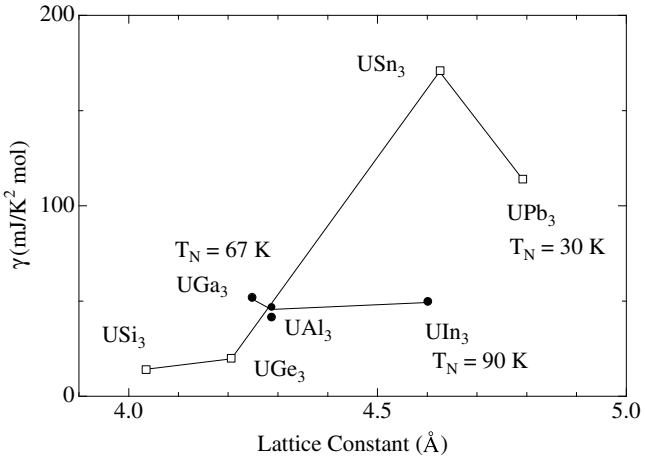

Figure 1. Hill plot for UX_3: γ versus the lattice constant.

2. Single crystal growth

High-quality single crystals are needed in the dHvA experiments. The single crystals were grown by the Czochralski-pulling method in a tetra-arc furnace for USi_3, UPt_3, UPd_2Al_3, UC, UGe_2 and $CeRh_2Si_2$, by the self-flux method for USn_3, UPb_3, $UPtGa_5$, USb_2, $CeCoIn_5$ and $CeAgSb_2$ and by the vapour transport method for UAs_2 and UP_2.

3. Experimental results and discussion

First we will discuss the Hill-plot rule for UX_3. UX_3 with the cubic $AuCu_3$-type structure, where X is an element of group IIIb (X: Al, Ga, In) or IVb (X: Si, Ge, Sn, Pb), exhibits a wide variety of magnetic properties including Pauli paramagnetism (USi_3 and UGe_3), spin fluctuations (USn_3 and UAl_3) and antiferromagnetism (UPb_3, UGa_3 and UIn_3). These different magnetic ground states are closely related to the lattice constant or the distance between U atoms and to hybridization of the 5f-electrons with the valence electrons. This is reflected in the electronic specific heat coefficient γ, which varies from 14 mJ K^{-2} mol^{-1} in USi_3 to 170 mJ K^{-2} mol^{-1} in USn_3 [2, 3]. When magnetic ordering occurs, the γ value is slightly reduced to 120 mJ K^{-2} mol^{-1} in UPb_3. The γ value in UX_3(IVb) series depends on the lattice constant, as shown in figure 1. The 5f-itinerant band model is well applicable to USi_3, UGe_3 and most likely USn_3 [2–4].

UX_3(IIIb) series compounds are very different from the UX_3(IVb) compounds, as shown in figure 1, although UAl_3 and UIn_3 approximately correspond to USn_3 and UPb_3, respectively. From this viewpoint, it can be suggested that an antiferromagnet UGa_3 is exceptional.

The compound UPt_3 is a typical spin fluctuation compound, which is now called a heavy fermion compound [5]. Heavy fermions in cerium compounds can be explained, simply, as follows [1, 6]. The 4f-levels of the Ce ion are generally split into three doublets in the crystal electric field (CEF) scheme at high temperatures because the 4f-electrons are mainly localized. At low temperatures, the magnetic entropy of the ground-state doublet in the 4f-levels is obtained by integrating C_m/T over the temperature. If the magnetic specific heat C_m is changed into the electronic one γT via the many-body Kondo effect, the γ value can be obtained as $\gamma = R \ln 2/T_K \simeq 10^4/T_K$ (mJ K^{-2} mol^{-1}). In fact, the γ value is 1600 mJ K^{-2} mol^{-1} in $CeCu_6$ for $T_K = 5$ K, and 350 mJ K^{-2} mol^{-1} in $CeRu_2Si_2$ for $T_K = 20$ K.

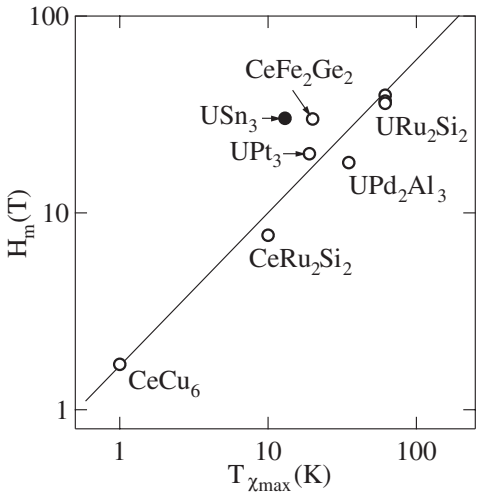

Figure 2. H_m versus $T_{\chi max}$ in uranium and cerium compounds.

Correspondingly the magnetic susceptibility χ increases with decreasing temperature, following the Curie–Weiss law, and possesses a maximum at a characteristic temperature $T_{\chi max}$. The magnetic susceptibility becomes constant at lower temperatures, indicating enhanced Pauli paramagnetism. This large susceptibility χ_0 correlates with the large γ value or the effective mass. $T_{\chi max}$ approximately corresponds to the Kondo temperature T_K. Usually the metamagnetic transition occurs at a magnetic field H_m ($g_{eff}\mu_B H_m = k_B T_{\chi max}$). Figure 2 shows the relationship between H_m and $T_{\chi max}$ in various cerium and uranium compounds [3].

We note that a large cyclotron mass of 100 m_0 (where m_0 is the rest mass of an electron) is detected in the dHvA experiment for UPt_3 [5], 65 m_0 in UPd_2Al_3 [7], 120 m_0 in $CeRu_2Si_2$ [8] and 100 m_0 in $CeCoIn_5$ [9], whereas the corresponding band mass is roughly one order smaller than the cyclotron mass. The mass enhancement based on the many-body Kondo effect is not included in the conventional band calculations. It is caused by spin fluctuations, where the freedom of the charge transfer of f-electrons appear in the form of an f-itinerant band, but the freedom of spin fluctuations of the same f-electrons reveals a relatively small magnetic moment and enhances the effective mass. A heavy fermion antiferromagnet UPd_2Al_3 with a magnetic moment of 0.85 μ_B/U, together with an antiferromagnet $UPtGa_5$ with 0.24 μ_B/U, are well explained by the energy band calculations based on the fully-relativistic spin-polarized linearized augmented-plane-wave method. Namely, 5f-electrons in these antiferromagnetically ordered uranium compounds are itinerant and also contribute to the magnetic moment at uranium sites.

Recently we have found quasi-two-dimensional Fermi surfaces in UX_2 (X: Bi, Sb, As, P), $CeTIn_5$ (T: Co, Rh, Ir) and $UTGa_5$ (T: Fe, Ni, Pt) [10, 11]. The present quasi-two-dimensionality is closely related to the magnetic unit cell and/or the unique crystal structure elongated along the tetragonal [001] direction, which bring about a flat Brillouin zone and produce cylindrical but corrugated Fermi surfaces along [001]. Figure 3 shows the angular dependence of the dHvA frequency $F(= \hbar c S_F/2\pi e)$, which is proportional to the extremal (maximum or minimum) cross-sectional area of the Fermi surface S_F. We simply assumed that all the dHvA branches correspond to cylindrical Fermi surfaces because the dHvA frequencies follow the $1/\cos\theta$-dependence, as shown by dotted curves.

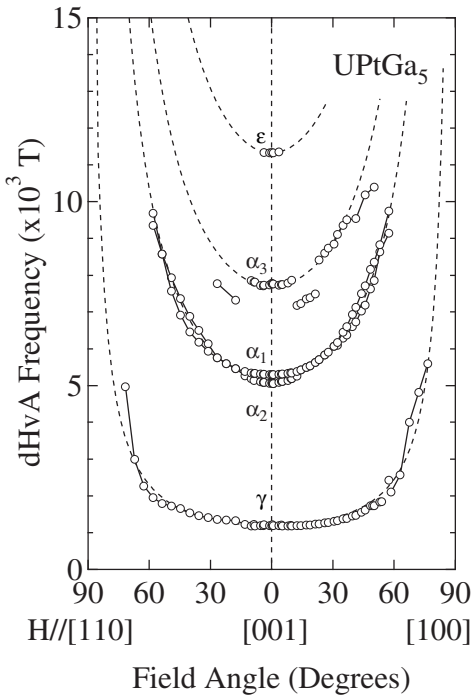

Figure 3. Angular dependence of the dHvA frequency in $UPtGa_5$.

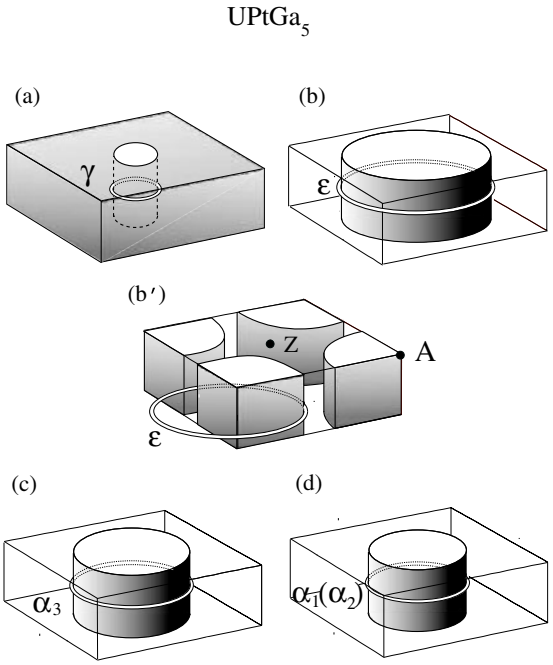

Figure 4. Fermi surfaces in $UPtGa_5$ obtained by the dHvA experiment.

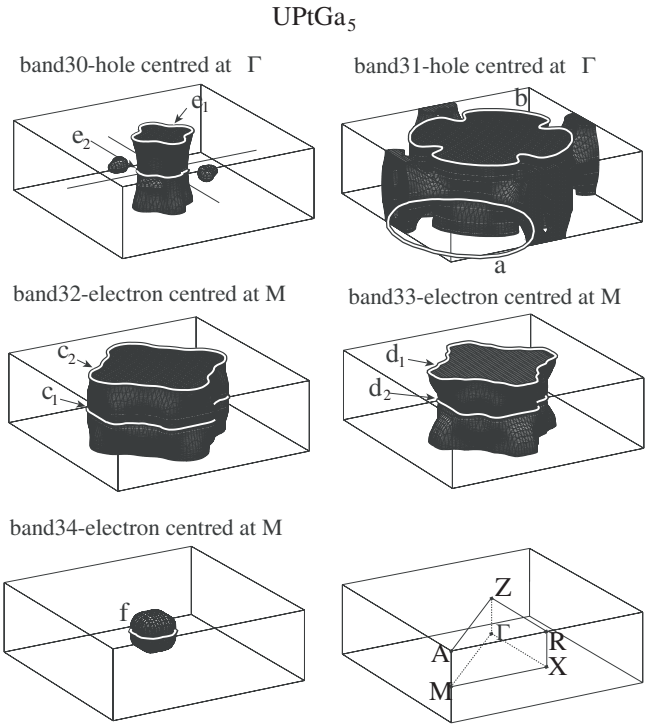

Figure 5. Fermi surfaces in $UPtGa_5$ obtained by the band calculation.

Figures 4 and 5 show the simple Fermi surface model obtained by the dHvA experiment and the corresponding theoretical Fermi surfaces, respectively. It is clear that branches ε, α_3, $\alpha_1(\alpha_2)$ and γ correspond to theoretical orbits a, $c_1(c_2)$, $d_1(d_2)$ and $e_1(e_2)$, respectively. Orbit f was not observed experimentally. The present spin-polarized band theory explains well the Fermi surface and the magnetic moment, where the spin and orbital moments are calculated as $-2.55\ \mu_B$/U and $2.84\ \mu_B$/U, respectively. The theoretical magnetic moment $0.29\ \mu_B$/U is in good agreement with the magnetic moment of $0.24\ \mu_B$/U determined from the neutron scattering experiment [12]. We note that the b-axis in the orthorhombic crystal structure of UGe_2 corresponds to the cylindrical axis. This is also related to the flat Brillouin zone along the b-axis because the b-axis is extremely long in this crystal structure [13].

The hybridization of the 5f-electrons with the valence electrons is usually uniform for all Fermi surfaces based on the cubic and hexagonal crystal structures. This is not applicable for small carrier systems or semimetals. A typical example is CeSb, which was once discussed with regard to the p–f mixing model [14]. We present here two typical compounds of UC and $CeAgSb_2$. The hole and electron Fermi surfaces in UC mainly originate from C 2p and U 5f, respectively. The cyclotron mass of the hole is low, being the rest mass of an electron m_0, while the mass of the electron is high, being in the range from 4 to 15 m_0 [15]. In a ferromagnet $CeAgSb_2$ with a small moment of $0.4\ \mu_B$/Ce, we have recently found a hollow cylindrical Fermi surface as shown in figure 6. Here $CeAgSb_2$ possesses a characteristic tetragonal crystal structure (P4/nmm) with the stacking arrangement of CeSb–Ag–CeSb–Sb layers along the [001] direction (c-axis) [16].

Finally we note the results of the dHvA experiments of UGe_2 and $CeRh_2Si_2$ under pressure. With increasing pressure, the Curie temperature $T_C = 52$ K in UGe_2 and the Néel temperature

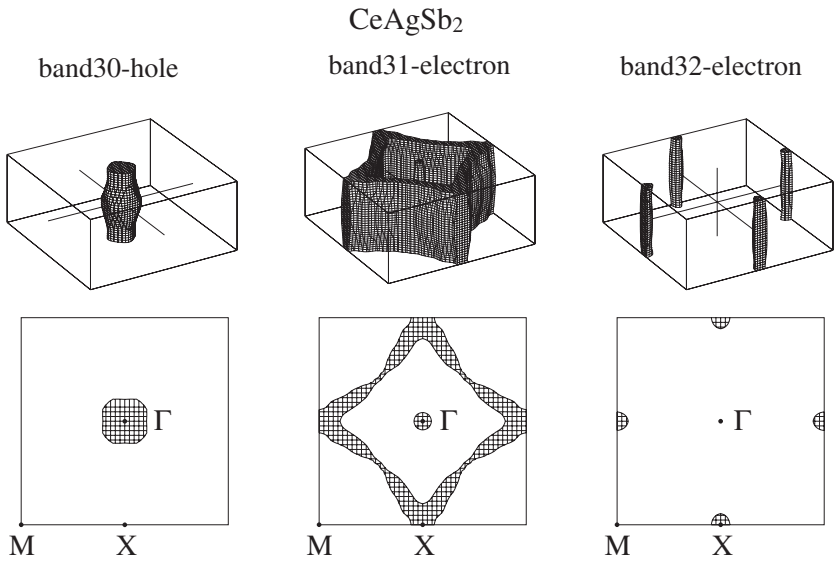

Figure 6. Fermi surfaces in $CeAgSb_2$.

$T_N = 36$ K in $CeRh_2Si_2$ decrease, and $T_C, T_N \to 0$ is reached at the critical pressures $P_c = 1.52$ and 1.06 GPa, respectively. The dHvA experiments indicate a discontinuous change of the Fermi surfaces in UGe_2 and $CeRh_2Si_2$ when the pressure crosses P_c [13].

4. Concluding remark

We have presented the Fermi surface property of uranium and cerium compounds via the dHvA experiment. The dHvA oscillations are usually observed in the normal state under high-field conditions, $\omega\tau \gg 1$, where $\omega_c (= eH/m_c^* c)$ is the cyclotron frequency and τ is the scattering lifetime. This phenomenon is observed even in the superconducting mixed state of several compounds such as $NbSe_2$, $CeRu_2$, UPd_2Al_3, URu_2Si_2 and $CeCoIn_5$ [9, 17, 18], but it is not clear why the dHvA oscillation is observed in low fields down to $H/H_{c2} = 0.2$–0.3. Here H_{c2} is the upper critical field in superconductivity. This question is open for future study.

Acknowledgment

This work was financially supported by Grant-in-Aid for COE Research (10CE2004) from the Ministry of Education, Culture, Sports, Science and Technology of Japan.

References

[1] Ōnuki Y, Goto T and Kasuya T 1991 *Materials Science and Technology* vol 3A, ed K H J Buschow (Weinheim: VCH) p 545
[2] Tokiwa Y, Harima H, Aoki D, Nojiri S, Murakawa M, Miyake K, Watanabe N, Settai R, Inada Y, Sugawara H, Sato H, Haga Y, Yamamoto E and Ōnuki Y 2000 *J. Phys. Soc. Japan* **69** 1105
[3] Sugiyama K, Iizuka T, Aoki D, Tokiwa Y, Miyake K, Watanabe N, Kindo K, Inoue T, Yamamoto E, Haga Y and Ōnuki Y 2002 *J. Phys. Soc. Japan* **71** 326
[4] Arko A J and Koelling D D 1978 *Phys. Rev.* B **17** 3104

[5] Kimura N, Tani T, Aoki H, Komatsubara T, Uji S, Aoki D, Inada Y, Ōnuki Y, Haga Y, Yamamoto E and Harima H 2000 *Physica* B **281/282** 710
[6] Ōnuki Y, Inada Y, Ohkuni H, Settai R, Kimura N, Aoki H, Haga Y and Yamamoto E 2000 *Physica* B **280** 276
[7] Inada Y, Yamagami H, Haga Y, Sakurai K, Tokiwa Y, Honma T, Yamamoto E, Ōnuki Y and Yanagisawa T 1999 *J. Phys. Soc. Japan* **68** 3643
[8] Aoki H, Uji S, Albessard A K and Ōnuki Y 1993 *Phys. Rev. Lett.* **71** 2110
[9] Settai R, Shishido H, Ikeda S, Murakawa Y, Nakashima M, Aoki D, Haga Y, Harima H and Ōnuki Y 2001 *J. Phys.: Condens. Matter* **13** L627
[10] Aoki D, Wísniewski P, Miyake K, Watanabe N, Inada Y, Settai R, Yamamoto E, Haga Y and Ōnuki Y 2000 *Phil. Mag.* B **80** 1517
[11] Ōnuki Y, Aoki D, Wísniewski P, Shishido H, Ikeda S, Inada Y, Settai R, Tokiwa Y, Yamamoto E, Haga Y, Maehira T, Harima H, Higuchi M, Hasegawa A and Yamagami H 2001 *Acta Phys. Pol.* B **32** 3273
[12] Tokiwa Y, Haga Y, Metoki N, Ishii Y and Ōnuki Y 2002 *J. Phys. Soc. Japan* **71** 725
[13] Araki S, Settai R, Nakashima M, Shishido H, Ikeda S, Nakawaki H, Haga Y, Tateiwa N, Kobayashi T C, Harima H, Yamagami H, Aoki Y, Namiki T, Sato H and Ōnuki Y 2002 *J. Phys. Chem. Solids* **63** 1133
[14] Settai R, Goto T, Sakatsume S, Kwon Y S, Suzuki T, Kaneta Y and Sakai O 1994 *J. Phys. Soc. Japan* **63** 3026
[15] Yamamoto E, Haga Y, Inada Y, Murakawa M, Ōnuki Y, Maehira T and Hasegawa A 1999 *J. Phys. Soc. Japan* **68** 3953
[16] Inada Y, Thamizhavel A, Yamagami H, Takeuchi T, Sawai Y, Ikeda S, Shishido H, Okubo T, Yamada M, Sugiyama K, Nakamura N, Yamamoto T, Kindo K, Ebihara T, Galatanu A, Yamamoto E, Settai R and Ōnuki Y 2002 *Phil. Mag.* B **82** 1867
[17] Inada Y and Ōnuki Y 1999 *Low Temp. Phys.* **25** 573
[18] Ohkuni Y, Inada Y, Tokiwa Y, Sakurai K, Settai R, Honma T, Haga Y, Yamamoto E, Ōnuki Y, Yamagami H, Takahashi S and Yanagisawa T 1999 *Phil. Mag.* B **79** 1045